Preston.[36] The analysis (neglecting second-order contributions) yields for Tc $C_s^2 = 0.0456$ and $C_d^2 = 0.69$, which corresponds to a $\beta^2$ value of $\beta^2 = 0.74$ ($C_s$ and $C_d$ are the Tc 5s and 4d contributions to the MO of the unpaired electron). The $\beta^2$ value is in good agreement with the one obtained above.

More insight in the bonding situation of $[TcOCl_5]^-$ and additional insight in that of the corresponding $[TcOX_5]^-$ complexes could be obtained if complexes with X = Br (the $^{79}Br^{81}Br$ hfs coupling constants are expected to be larger by a factor 4 or 5 than the $^{35}Cl^{37}Cl$ splittings because of the larger nuclear magnetic moments of $^{79}Br^{81}Br$) would be available. However, when the same reaction conditions as those used for $[TcOCl_5]^-$ were applied (using a concentrated solution of HBr instead of HCl), the formation of $[TcOBr_5]^-$ could not be detected.

Finally, it should be noted that the complex anion $[TcOCl_5]^-$ formed by the reaction of $[TcO_4]^-$ with $H_2SO_4$/HCl is not stable for a longer time; after 1 h the deep blue color of the solution vanishes and the intensity of the EPR signal decreases.

**Acknowledgment.** The authors thank Prof. Dr. I. N. Marov (Vernadsky-Institute, Academy of Sciences, Moscow) for stimulating this work.

**Registry No.** $KTcO_4$, 13718-33-7; $[TcOCl_5]^-$, 93558-25-9.

(36) Morton, J. R.; Preston, K. F. *J. Magn. Reson.* **1978**, *30*, 577.

Contribution from the P. M. Gross Chemical Laboratory, Department of Chemistry, Duke University, Durham, North Carolina 27706

# Comparison of the Kinetics, Mechanism, and Thermodynamics of Aqueous Iron(III) Chelation and Dissociation by Hydroxamic Oxo and Thio Acid Ligands

L. LYNNE FISH and ALVIN L. CRUMBLISS*

*Received July 17, 1984*

The kinetics and thermodynamics of aqueous iron(III) complexation by 4-$CH_3OC_6H_4C(X)N(OH)H$ (X = O, S) to form $Fe(H_2O)_4(4\text{-}CH_3OC_6H_4C(X)N(O)H)^{2+}$ are reported. These data provide a direct comparison between the iron(III) chelation chemistry of hydroxamic oxo and thio acids. A parallel-path mechanism involving $Fe(H_2O)_6^{3+}$ and $Fe(H_2O)_5OH^{2+}$ was found to be operative for both ligands. Equilibrium quotients and microscopic rate constants for the forward and reverse directions of both paths were obtained along with the corresponding $\Delta H°$, $\Delta H^*$ and $\Delta S°$, $\Delta S^*$ values. An associative interchange ($I_a$) mechanism is operative for the substitution of both ligands at $Fe(H_2O)_6^{3+}$. Data are also presented that support an $I_a$ mechanism for substitution at $Fe(H_2O)_5OH^{2+}$, although the associative character in this path may be due to H-bonding interactions between the ligand and coordinated $OH^-$. Initial bond formation at iron(III) for either path occurs at the >C=X (X = O, S) site. The *thio*hydroxamic acid forms a more stable complex at physiological pH, and aquation by the acid-dependent and acid-independent paths is ca. 50 times slower than for the hydroxamic acid complex. The increased kinetic stability is consistent with enhanced delocalization of the N atom lone electron pair into the C-N bond in the thiohydroxamic acid complex. The chemistry of iron(III) chelation by $CH_3OC_6H_4C(S)N(OH)H$ suggests that siderophores may exist that use the thiohydroxamate moiety for iron(III) binding.

## Introduction

Siderophores are low molecular weight sequestering agents synthesized by microbes to facilitate the solubilization and transport of iron from the environment to the cell. The structure and function of these natural chelators have been reviewed.[1-4] An important structural feature of the siderophores is the incorporation of catechol or hydroxamate groups that are capable of selectively binding iron(III) in the presence of other biologically important metal ions.[5] Synthetic catechol and hydroxamic acid chelators have been investigated as structural and kinetic models of the siderophores.[6-9] An investigation of the electronic effects influencing hydroxamic acid-iron(III) chelation kinetics and complex stability is being carried out in this laboratory.[10-12]

Closely related to the hydroxamic acids are the *thio*hydroxamic acids, $R_1C(S)N(OH)R_2$,[13] which are also capable of forming stable transition-metal complexes.[14] Cupric and ferric complexes of *N*-methylthioformohydroxamic acid have been isolated from the culture supernatant fluids of *Pseudomonas fluorescens*,[15] *Pseudomonas reptilivora*,[16] and *Streptomyces*.[17] Although the biological function of these thiohydroxamato complexes is not fully understood, they have been found to exhibit antibiotic activity,[15-18] which is a characteristic of several hydroxamic acid siderophores.[19]

(1) (a) Neilands, J. B. *Microbiol. Sci.* **1984**, *1*, 9. (b) Neilands, J. B. *Adv. Inorg. Biochem.* **1983**, *5*, Chapter 6. (c) Neilands, J. B. *Annu. Rev. Microbiol.* **1982**, *36*, 285. (d) Neilands, J. B. *Annu. Rev. Biochem.* **1981**, *50*, 715. (e) Neilands, J. B. In "Iron in Biochemistry and Medicine", 2nd ed.; Jacobs, A., Worwood, M., Eds.; Academic Press: New York, 1980; p 529.
(2) (a) Emery, T. *Am. Sci.* **1982**, *70* (6), 626. (b) Emery, T. *Met. Ions Biol. Syst.* **1978**, *1*, Chapter 3.
(3) (a) Raymond, K. N.; Müller, G.; Matzanke, B. F. *Top. Curr. Chem.* **1984**, *123*, 49. (b) Raymond, K. N.; Carrano, C. J. *Acc. Chem. Res.* **1979**, *12*, 183.
(4) Messenger, A. J. M.; Barclay, R. *Biochem. Educ.* **1983**, *11*, 54.
(5) Neilands, J. B.; Ratledge, C. In "Handbook of Microbiology"; Laskin, A. I., Lechevalier, H. A., Eds.; CRC Press: Boca Raton, FL, 1982; Vol. IV, p 565.
(6) (a) Raymond, K. N.; Tufano, T. P. In "The Biological Chemistry of Iron"; Dunford, H. B., Dolphin, D., Raymond, K. N., Sieker, L., Eds.; D. Reidel Publishing Co.: Boston, 1982; p 85. (b) Raymond, K. N.; Pecoraro, V. L.; Weitl, F. L. In "Development of Iron Chelators for Clinical Use"; Martell, A. E., Anderson, W. F., Badman, D. G., Eds.; Elsevier: New York, 1981; p 165. (c) Raymond, K. N.; Abu-Dari, K.; Sofen, S. R. *ACS Symp. Ser.* **1980**, *No. 119*, 133.
(7) (a) Birus, M.; Kujundzič, N.; Pribanič, M. *Inorg. Chim. Acta* **1980**, *55*, 65. (b) Kujundzič, N.; Pribanič, M. *J. Inorg. Nucl. Chem.* **1978**, *40*, 789.
(8) Kazmi, S. A.; McArdle, J. V. *J. Inorg. Nucl. Chem.* **1981**, *43*, 3031.
(9) Brown, D. A.; Chidambaram, M. B. In "Metal Ions in Biological Systems"; Sigel, H., Ed.; Marcel Dekker: New York, 1982; Vol. 14, Chapter 5.
(10) Monzyk, B.; Crumbliss, A. L. *J. Am. Chem. Soc.* **1979**, *101*, 6203.
(11) Monzyk, B.; Crumbliss, A. L. *J. Inorg. Biochem.* **1983**, *19*, 19.
(12) Brink, C. P.; Crumbliss, A. L. *Inorg. Chem.* **1984**, *23*, 4708.
(13) Walter, W.; Schaumann, E. *Synthesis* **1971**, *No. 3*, 111.
(14) Mizukami, S.; Nagata, K. *Coord. Chem. Rev.* **1968**, *3*, 267.
(15) (a) Itoh, S.; Inuzuka, K.; Suzuki, T. *J. Antibiot.* **1970**, *23*, 542. (b) Shirahata, T.; Deguchi, T.; Hayashi, T.; Matsubora, I.; Suzuki, T. *J. Antibiot.* **1970**, *23*, 546. (c) Egawa, Y.; Umino, K.; Awataguchi, S.; Kawano, Y.; Okuda, T. *J. Antibiot.* **1970**, *23*, 267.
(16) (a) Del Rio, L. A.; Gorgé, J. C.; Olwares, J.; Mayor, F. *Antimicrob. Agents Chemother.* **1972**, *2*, 189. (b) Martinez-Molina, E.; Del Rio, L. A.; Olivares, J. *J. Appl. Bacteriol.* **1976**, *41*, 69.
(17) Miyamura, S. Japanese Patent 87 087, 1973.
(18) Bell, S. J.; Friedman, S. A.; Leong, J. *Antimicrob. Agents Chemother.* **1979**, *15*, 384.
(19) Neilands, J. B. *Adv. Chem. Ser.* **1977**, *No. 162*, 3.

0020-1669/85/1324-2198$01.50/0 

The formation of stable five-membered chelate rings with iron(III) that are structurally similar to the hydroxamic acids[20,21] suggests a possible siderophore role for natural chelators that possess the thiohydroxamic acid functional group. As a test of the chemical basis for this hypothesis we report here a direct comparison of the kinetic and thermodynamic behavior of a mono(*thio*-hydroxamato)iron(III) (X = S) complex with the corresponding mono(hydroxamato)iron(III) (X = O) complex as shown in I. This investigation also allows us to further probe the intimate mechanism of ligand substitution at high-spin aqueous iron(III).

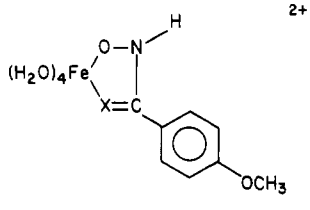


I: X = O, S

## Experimental Section

**Materials.** Iron(III) perchlorate (G. F. Smith) was recrystallized twice from dilute perchloric acid before use. Sodium perchlorate was prepared by neutralization of $Na_2CO_3$ (Fisher, ACS Certified) by $HClO_4$ (Mallinckrodt) and was recrystallized from water prior to use. All solutions were prepared with water distilled once from acidic $K_2Cr_2O_7$ and then slowly from basic $KMnO_4$ in an all-glass apparatus with Teflon sleeves and stopcocks. Hydroxylamine hydrochloride (Aldrich), *p*-anisoyl chloride (Aldrich), *p*-bromoanisole (Aldrich), carbon disulfide (Aldrich), and chloroacetic acid (Aldrich) were used without further purification. 4-Methoxybenzohydroxamic acid was prepared as described previously;[22] mp 161–162 °C (lit. mp 163 °C).[23] Anal. Found (calcd): C, 57.51 (57.48); H, 5.32 (5.42); N, 8.53 (8.38). 4-Methoxybenzothiohydroxamic acid was prepared by an adaptation of a literature method;[24] mp 117–118 °C (lit. mp 117–118 °C).[24] Anal. Found (calcd): C, 52.53 (52.45); H, 5.05 (4.95); N, 7.69 (7.65); S, 17.47 (17.50).

**Methods. Equilibrium Measurements.** Mono(hydroxamato)iron(III) complex formation constants, $Q_f$, were obtained from static absorbance measurements at 25 °C. Data were collected at conditions such that there was 5–100% complex formation: $[H^+] = 0.1$ M, $I = 2.0$ M ($NaClO_4/HClO_4$), [Fe(III)]/[HA] = 0.3–190. The solutions were made by addition of acid first, then the calculated volume of the stock Fe(III) solution, and finally a constant volume of a stock ligand solution prepared by dissolving the ligand in 2.0 M $NaClO_4$ solution. The solutions were then diluted with 2.0 M $NaClO_4$. Preparation and standardization of the stock iron(III) solutions and stock $NaClO_4$ solutions used in all of the kinetic and equilibrium studies have been previously described.[10,12] The iron(III) and ligand solutions were delivered from a Gilmont ultraprecision micrometer buret capable of 0.0001-mL precision. Spectral data were collected over the wavelength range from 400 to 700 nm ($\lambda_{max}$ = 540 nm, $\epsilon = 1586$ $M^{-1}$ $cm^{-1}$) to demonstrate a wavelength independence for the calculated formation constants. A single equilibrium is established for the mono(hydroxamato)iron(III) complex formation (reaction 4) such that the formation quotient, $Q_f$, is defined by eq 1, where HA

$$Q_f = [Fe(H_2O)_4A^{2+}][H^+]/[Fe(H_2O)_6^{3+}][HA] \quad (1)$$

represents $CH_3OC_6H_4C(O)N(OH)H$. The mono complex $Fe(H_2O)_4A^{2+}$ was established as the sole absorbing species by matrix methods.[25] Consequently, the formation constant, $Q_f$, may be computed from absorbance data by the equation (2), where $Abs_e$ is the equilibrium ab-

$$\frac{(Abs_e/l\epsilon)[H^+]}{[H^+]_{tot} - Abs_e/l\epsilon} = Q_f\{[Fe(III)]_{tot} - Abs_e/l\epsilon\} \quad (2)$$

sorbance, $[Fe(III)]_{tot}$ is the total free and complexed iron(III) concentration, $[HA]_{tot}$ is the total free and complexed hydroxamic acid concentration, $\epsilon$ is the molar extinction coefficient for $Fe(A)(H_2O)_4^{2+}$, and $l$ is the light path length.

Infinite time absorbance readings from kinetic experiments over the temperature range from 20 to 45 °C were used in order to calculate $\Delta H_f°$ and $\Delta S_f°$ values from plots of ln $Q_f$ vs. $1/T$, where $Q_f$ values at each temperature were computed from eq 3. In these experiments the [Fe(III)]/[HA] ratio was fixed ([Fe(III)] = [HA] = $C_{tot} = 5 \times 10^{-4}$ M) and the $[H^+]$ varied over the range from 0.025 to 1.00 M.

$$C_{tot}/Abs_e = ([H^+]/Abs_e)^{1/2}/(l\epsilon Q_f)^{1/2} + 1/l\epsilon \quad (3)$$

Data for the mono(thiohydroxamato)iron(III) complex formation constant, $Q_f$, determinations were obtained from static absorbance measurements in 5% MeOH solutions. Reagent mono(thiohydroxamato)iron(III) complex solutions were prepared by diluting the stock iron(III) solution with $HClO_4/NaClO_4$ (adding acid first) and then adding a fixed amount of a stock thiohydroxamic acid (HSA) solution. The HSA solution was prepared by dissolving the ligand in MeOH and then diluting with aqueous $NaClO_4$. The amount of MeOH used is such that when an aliquot of the HSA solution was added to the Fe(III)/$HClO_4$ mixture, the resulting solution was 5% MeOH. These solutions were prepared so that [Fe(III)] = (2–3.5) $\times 10^{-4}$ M, [HSA] = $2 \times 10^{-4}$ M, $[HClO_4] = 0.29$ or 0.87 M, and $I = 2.0$ M ($NaClO_4$). These conditions lead to a [Fe(III)]/[HSA] ratio from 1 to ca. 2, which corresponds to between 60 and 90% complexation. These absorbance measurements were made over a temperature range from 20 to 40 °C in the region from 400 to 700 nm ($\lambda_{max}$ = 470 nm, $\epsilon = 1355$ $M^{-1}$ $cm^{-1}$). Formation constants, $Q_f$, were calculated from appropriate plots of eq 2 at each temperature and $\Delta H_f°$ and $\Delta S_f°$ values obtained from plots of ln $Q_f$ vs. $1/T$.

**Kinetic Measurements.** An Aminco stopped-flow apparatus equipped with computerized data acquisition and temperature control systems was used as described previously.[10,12]

Relaxation kinetic data for the $Fe(H_2O)_6^{3+}$/4-methoxybenzohydroxamic acid system were obtained by flowing together the reagent solution ([Fe(III)] = [HA] $\approx 10^{-3}$ M, $[HClO_4] = 0.01$ M, $[ClO_4^-] = 2.0$ M ($NaClO_4$)) with a solution of increased acid concentration ($[HClO_4]$ = 0.05–2.0 M, $[ClO_4^-] = 2.0$ M ($NaClO_4$)). Each experimental relaxation rate constant reported represents 50–60 data points from three to five separate stopped-flow injections.

Pseudo-first-order kinetic data used in the study of the thiohydroxamic acid system were obtained by flowing together a thiohydroxamic acid solution and an iron(III) solution ([Fe(III)]/[HSA] ≥ 10) where both the iron and ligand solution were of the same $[HClO_4]$ (from 0.06 to 0.8 M). Reagent thiohydroxamic acid solutions were prepared by dissolving the ligand in the appropriate amount of MeOH to make the final solution 5% MeOH by volume. The ligand solution was then diluted with $HClO_4/NaClO_4$ such that $I = 2.0$ M and $1.0 \times 10^{-4}$ M < [HSA] < $2.4 \times 10^{-4}$ M for [Fe(III)] dependency kinetic trials and [HSA] = $2.4 \times 10^{-4}$ M for $[H^+]$ dependency kinetic trials where the calculated $[H^+]$ = 0.06–0.8 M. Reagent iron(III) solutions for pseudo-first-order kinetic trials were prepared by dilution of the stock solution with aqueous $HClO_4/NaClO_4$ (adding acid first) so that $10^{-3}$ M < [Fe(III)] < $10^{-2}$ M for [Fe(III)] dependency trials and [Fe(III)] = $2.4 \times 10^{-3}$ M for $[H^+]$ dependency trials. Solutions were prepared so that $[HClO_4] = 0.06$–0.8 M and $I = 2.0$ M ($NaClO_4$). For consistency with the ligand solutions, solutions were made to be 5% MeOH by volume. Data were first obtained for a range of [Fe(III)] ($5 \times 10^{-4}$ to $5 \times 10^{-3}$ M) to determine [Fe(III)] dependence and for five $[HClO_4]$ over a range from 0.06 to 0.8 M to determine $[H^+]$ dependence. The $[H^+]$ dependence trials were carried out at five temperatures from 20 to 40 °C.

A limited amount of data was collected for the hydroxamic acid system at the same pseudo-first-order conditions as were used for the thiohydroxamic acid system in both aqueous and 5% MeOH solution at 25 °C. These experiments were performed in order to establish the validity of a direct comparison of the results obtained for the hydroxamic oxo and thio acid systems. Reagent hydroxamic acid solutions in 5% MeOH for the pseudo-first-order kinetic trials were prepared as described for the thiohydroxamic acid system. For the $[H^+]$ dependency kinetic trial, $[HA] = 2.4 \times 10^{-4}$ M, $[H^+] = 0.06$–0.8 M, and $I = 2.00$ M ($NaClO_4$), while for the [Fe(III)] dependency kinetic trials [HA] = (1–2.4) $\times 10^{-4}$ M, $[H^+] = 0.316$ M, and $I = 2.00$ M. Reagent iron solutions were prepared as previously stated, but [Fe(III)] dependency kinetic trials were performed only at 0.316 M ($HClO_4$). To determine the effect of MeOH, a $[H^+]$ dependency kinetic trial was also performed without MeOH present.

## Results

**Equilibrium Studies.** Previous work in our laboratory[10,12] has shown that for the hydroxamic acid ligand the only absorbing species present at the conditions of our equilibrium and kinetic

(20) Freyberg, D. P.; Abu-Dari, K.; Raymond, K. N. *Inorg. Chem.* **1979**, *18*, 3037.
(21) (a) Murray, K. S.; Newman, P. J.; Taylor, D. *J. Am. Chem. Soc.* **1978**, *100*, 2251. (b) Murray, K. S.; Newman, P. J.; Gatehouse, B. M.; Taylor, D. *Aust. J. Chem.* **1978**, *31*, 983.
(22) Brink, C. P.; Fish, L. L.; Crumbliss, A. L. *J. Org. Chem.*, in press.
(23) Hackeley, B. E.; Plapinger, R.; Stolberg, M. *J. Am. Chem. Soc.* **1955**, *77*, 3651.
(24) (a) Jensen, K. A.; Buchardt, O.; Christophersen, C. *Acta Chem. Scand.* **1967**, *21*, 1936. (b) Mitchell, A. J.; Murray, K. S.; Newman, P. J.; Clark, P. E. *Aust. J. Chem.* **1977**, *30*, 2439.
(25) Coleman, J. S.; Varga, L. P.; Mastin, S. H. *Inorg. Chem.* **1970**, *9*, 1015.

Table I. Thermodynamic Data for Mono(hydroxamato)iron(III) Complex Formation

| | $CH_3OC_6H_4$-C(O)N(OH)H | $CH_3OC_6H_4$-C(S)N(OH)H |
|---|---|---|
| | Reaction 4 | |
| $10^{-2}Q_f$ (25 °C) | 2.49 (0.01) | 88.8 (1.6) |
| $\Delta H_f^\circ$,[a] kcal/mol | 3.1 (0.2) | 9.1 (1.5) |
| $\Delta S_f^\circ$,[a] cal/(K mol) | 20 (1) | 48 (5) |
| | Reaction 5 | |
| $10^{-8}Q_f'$,[b] $M^{-1}$ (25 °C) | 1430 | 7.91 |
| $\Delta H_f^{\circ\prime}$,[c] kcal/mol | −2.5 | |
| $\Delta S_f^{\circ\prime}$,[c] cal/(K mol) | 41 | |
| | Reaction 9 | |
| $10^{-5}Q_f''$,[d] $M^{-1}$ (25 °C) | 1.62 | 54.1 |
| $\Delta H_f^{\circ\prime\prime}$,[e] kcal/mol | −7.2 | −1.1 |
| $\Delta S_f^{\circ\prime\prime}$,[e] cal/(K mol) | −1 | 27 |

[a] $\Delta H_f^\circ$ and $\Delta S_f^\circ$ for reaction 4 obtained from the slopes and intercepts of plots of ln $Q_f$ vs. $1/T$ over the temperature range from 20 to 40 °C. [b] Formation quotient for reaction 5 calculated according to $Q_f' = Q_f/K_a$ at 25 °C, where the ligand acidity constants, $K_a$, were obtained from ref 22 and 26. Estimated errors for the calculated values 2%. [c] $\Delta H_f^{\circ\prime}$ and $\Delta S_f^{\circ\prime}$ for reaction 5 calculated from $\Delta H_f^\circ$ and $\Delta S_f^\circ$ for reaction 4 and $\Delta H_a^\circ$ and $\Delta S_a^\circ$ for acid dissociation obtained from ref 22. [d] Formation quotient for reaction 9 calculated according to $Q_f'' = Q_f/K_h$ at 25 °C, where the hydrolysis constant $K_h$ was obtained from ref 27. Estimated errors for the calculated values 2%. [e] $\Delta H_f^{\circ\prime\prime}$ and $\Delta S_f^{\circ\prime\prime}$ for reaction 9 calculated according to the relationships $\Delta H_f^{\circ\prime\prime} = \Delta H_f^\circ - \Delta H_h$ and $\Delta S_f^{\circ\prime\prime} = \Delta S_f^\circ - \Delta S_h$. $\Delta H_h$ and $\Delta S_h$ values obtained from ref 27.

measurements is the mono(hydroxamato)iron(III) complex. We have observed that the bis and tris complexes form more readily for the thiohydroxamic acid ligand. Therefore, matrix methods[25] were used to establish that when [Fe(III)]/[HSA] ≥ 1 and [$H^+$] = 0.95–$10^{-3}$ M (5% MeOH), only one light-absorbing species, the mono(thiohydroxamato)iron(III) complex, is present. These observations and the acidity constants of the two ligands investigated[22,26] establish that the reaction described in this kinetic and equilibrium study at low pH is that shown in eq 4, where X = S or O.

$$Fe(H_2O)_6^{3+} + CH_3OC_6H_4C(X)N(OH)H \overset{Q_f}{\rightleftharpoons} Fe(H_2O)_4(CH_3OC_6H_4C(X)N(O)H)^{2+} + H_{aq}^+ + H_2O \quad (4)$$

The equilibrium quotient, $Q_f$, for this reaction was calculated along with the corresponding $\Delta H_f^\circ$ and $\Delta S_f^\circ$ values as described in the Experimental Section. These values are listed in Table I. Values for $Q_f''$ and the corresponding $\Delta H_f^{\circ\prime\prime}$ and $\Delta S_f^{\circ\prime\prime}$ values were computed for reaction 9 in Scheme I from the literature values for the $Fe(H_2O)_6^{3+}$ hydrolysis constant, $K_h$.[27] Values for the equilibrium quotient for reaction 5 ($Q_f'$), which was not directly observed, were obtained from ligand p$K_a$ values. These are listed in Table I along with the corresponding $\Delta H_f^{\circ\prime}$ and $\Delta S_f^{\circ\prime}$ values.

$$Fe(H_2O)_6^{3+} + CH_3OC_6H_4C(X)N(O)H^- \overset{Q_f'}{\rightleftharpoons} Fe(H_2O)_4(CH_3OC_6H_4C(X)N(O)H)^{2+} + 2H_2O \quad (5)$$

**Kinetics.** Relaxation kinetic studies for the $Fe(H_2O)_6^{3+}$/$CH_3OC_6H_4C(O)N(OH)H$ system were carried out as previously described[10,12] by rapidly increasing the [$H^+$] of an iron(III)/hydroxamic acid complex solution (where [Fe(III)] = $[HA]_{tot}$) from 0.01 to 0.025–1.00 M. This results in the measurement of a first-order rate constant, $k^{rel}_{exptl}$, which corresponds to the relaxation to a new equilibrium position. Table II is a compilation of the first-order relaxation rate constants determined as a function of [$H^+$] from 20 to 40 °C.[28] Figure 1 is a representative plot of these data at 25 °C. The solid line represents a least-squares fit of eq 6 to the experimental data. A good fit of eq 6 to the relaxation rate constants was obtained for each temperature data set given in Table II.[28]

$$k^{rel}_{exptl} = a + b/[H^+] + c[H^+] \quad (6)$$

A simple parallel-path mechanism is presented in Scheme I, which takes into account the single $Fe_{aq}^{3+}$ hydrolysis product present at our conditions. A reaction path involving the hydroxamate anion may be neglected due to the high p$K_a$ value of the acid and the low pH conditions of our study. Furthermore, inclusion of such a path results in a calculated second-order rate constant close to the diffusion-controlled value, which is unreasonable for $Fe_{aq}^{3+}$. It has been shown[10] that when Scheme I is treated as a relaxation process at the conditions where $[Fe(III)]_{tot} = [HA]_{tot} = C_{tot}$ and $2k_1$ ($C_{tot} - [Fe(H_2O)_4A^{2+}]_e$) is small, then the equation (10) may be derived for the relaxation rate constant

Table III. Kinetic Parameters Corresponding to Scheme I

| | $CH_3OC_6H_4$-C(O)N(OH)H[a] | $CH_3OC_6H_4$-C(S)N(OH)H[b] |
|---|---|---|
| $k_1/M^{-1}\ s^{-1}$ (25 °C) | 4.7 | 3.3 (0.4) |
| $\Delta H_1^\ddagger$/kcal/mol | 14.0 | 19.1 (3.1) |
| $\Delta S_1^\ddagger$/cal/(K mol) | −9 | 8 (10) |
| $10^{-3}k_2/M^{-1}\ s^{-1}$ | 2.5 | 3.8 (0.03) |
| $\Delta H_2^\ddagger$/kcal/mol | 3.0 (0.8) | 6.7 (0.5) |
| $\Delta S_2^\ddagger$/cal/(K mol) | −33 (3) | −20 (2) |
| $10^2k_{-1}/M^{-1}\ s^{-1}$ | 1.9 | 0.039 |
| $\Delta H_{-1}^\ddagger$/kcal/mol | 11.1 (0.9) | 13.1 (1.7) |
| $\Delta S_{-1}^\ddagger$/cal/(K mol) | −29 (3) | −30 (6) |
| $10^2k_{-2}/s^{-1}$ | 2.9 | 0.070 |
| $\Delta H_{-2}^\ddagger$/kcal/mol | 19.7 (0.3) | 9.5 (1.3) |
| $\Delta S_{-2}^\ddagger$/cal/(K mol) | 0 (1) | −41 (4) |

[a] Rate constants $k_2$, $k_{-2}$, and $k_{-1}$ calculated from $k^{rel}_{exptl}$ values (Table II)[28] obtained at 25 °C from eq 11. Associated activation parameters obtained from $k_2$, $k_{-2}$, and $k_{-1}$ values calculated at 20, 25, 30, 35, and 40 °C from $k^{rel}_{exptl}$ values (Table II) and plotted as ln $(k/T)$ vs. $1/T$. Rate constant $k_1$ calculated from $k_1 = Q_f k_{-1}$. $\Delta H_1^\ddagger$ and $\Delta S_1^\ddagger$ calculated from $\Delta H_f^\circ$, $\Delta S_f^\circ$ (Table I) and $\Delta H_{-1}^\ddagger$, $\Delta S_{-1}^\ddagger$ values. Rate constant values reproducible to within 3% with all data at $I$ = 2.00 M ($NaClO_4/HClO_4$). [b] All data collected at $I$ = 2.00 M ($NaClO_4/HClO_4$) and 5% MeOH/$H_2O$. Rate constants $k_1$ and $k_2$ obtained from the intercept and slope, respectively, of Figure 4. Associated activation parameters obtained from plots of ln $(k/T)$ vs. $T^{-1}$ at 20, 25, 30, 35, and 40 °C. Rate constants $k_{-1}$ and $k_{-2}$ calculated from the relations $k_{-1} = k_1/Q_f$ and $k_{-2} = k_2/Q_f''$, respectively. Estimated errors 10%. $\Delta H^\ddagger$ and $\Delta S^\ddagger$ values for the reverse reactions calculated from ln $(k/T)$ vs. $1/T$ plots.

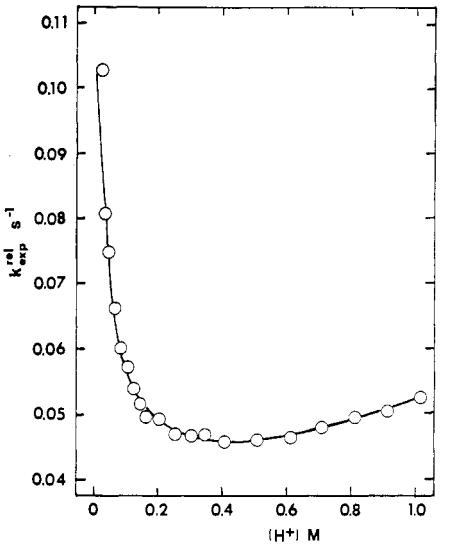


**Figure 1.** Plot of $k^{rel}_{exptl}$ vs. [$H^+$] for the $Fe(H_2O)_4(CH_3OC_6H_4C(O)N(O)H)^{2+}$ system at 25 °C. Each data point represents three to five independent determinations of $k^{rel}_{exptl}$. Standard deviations are smaller than the data point size. The solid line represents a least-squares fit of eq 6 and 10 to the data. See Table II for data.[28] Conditions: [Fe(III)] = [HA] = 5 × $10^{-4}$ M, $I$ = 2.00 M ($NaClO_4/HClO_4$).

(26) Nagata, K.; Mizukami, S. *Chem. Pharm. Bull.* **1966**, *14*, 1255.
(27) (a) Siddall, T. H., III; Vosburgh, W. C. *J. Am. Chem. Soc.* **1951**, *73*, 4270. (b) Milburn, R. M. *J. Am. Chem. Soc.* **1957**, *79*, 537.
(28) See paragraph at end of paper regarding supplementary material.

Scheme I[a]

$$\text{path 1: } Fe(H_2O)_6^{3+} + CH_3OC_6H_4C(X)N(OH)H \underset{k_{-1}}{\overset{Q_f,\ k_1}{\rightleftharpoons}} Fe(H_2O)_4(CH_3OC_6H_4C(X)N(O)H)^{2+} + H_{aq}^{+} + 2H_2O \quad (7)$$

$$-H^+ \Big\downarrow \Big\uparrow H^+ \qquad K_h \quad (8)$$

$$\text{path 2: } Fe(H_2O)_5OH^{2+} + CH_3OC_6H_4C(X)N(OH)H \underset{k_{-2}}{\overset{Q_f'',\ k_2}{\rightleftharpoons}} Fe(H_2O)_4(CH_3OC_6H_4C(X)N(O)H)^{2+} + 2H_2O \quad (9)$$

[a] X = O, S.

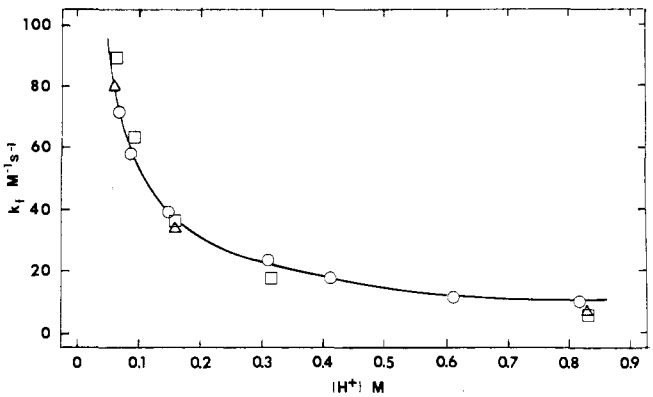


**Figure 2.** Plot of the macroscopic rate constant for the formation of $Fe(H_2O)_4(CH_3OC_6H_4C(O)N(O)H)^{2+}$ vs. $[H^+]$ at 25 °C; O, data obtained from the relaxation kinetic study, $k_f = (k^{rel}_{exptl} - k_{-2} - k_{-1}[H^+])/[Fe(III)]$ ($[Fe(III)] = [HA] = 5.0 \times 10^{-4}$ M, $I = 2.00$ M ($NaClO_4/HClO_4$)); Δ, data obtained from the pseudo-first-order kinetic study, $k_f = (k_{obsd} - k_{-2} - k_{-1}[H^+])/[Fe(III)]$ ($[Fe(III)] = 1.2 \times 10^{-3}$ M, $[HA] = 1.2 \times 10^{-4}$ M, $I = 2.00$ M ($NaClO_4/HClO_4$)); □, data obtained from the pseudo-first-order kinetic study, $k_f = (k_{obsd} - k_{-2} - k_{-1}[H^+])/[Fe(III)]$ ($[Fe(III) = 1.2 \times 10^{-3}$ M, $[H] = 1.2 \times 10^{-4}$ M, $I = 2.00$ M ($NaClO_4/HClO_4$), 5% $MeOH/H_2O$). In each case $k_{-2}$ and $k_{-1}$ values used were those obtained from relaxation studies.

$k^{rel}_{exptl}$. This equation is of the same form as the empirical eq

$$k^{rel}_{exptl} = k_{-2} + (2k_2K_h(C_{tot} - [Fe(H_2O)_4A^{2+}]_e))/[H^+] + k_{-1}[H^+] \quad (10)$$

6, where $a = k_{-2}$, $b = 2k_2K_h(C_{tot} - [Fe(H_2O)_4A^{2+}]_e)$, and $c = k_{-1}$; the quantity $[Fe(H_2O)_4A^{2+}]_e$ is calculated at each $[H^+]$ from equilibrium absorbance measurements.[28] Values for the rate constants $k_2$, $k_{-2}$, and $k_{-1}$ calculated at each temperature were obtained from a least-squares fit of eq 10, rearranged as shown in eq 11, by using experimental values for $k^{rel}_{exptl}$, $[H^+]$, $Abs_e$, $C_{tot}$,

$$k^{rel}_{exptl}[H^+] = 2k_2K_h(C_{tot} - [Fe(H_2O)_4A^{2+}]_e) + k_{-2}[H^+] + k_{-1}[H^+]^2 \quad (11)$$

and $\epsilon$[28] and literature values for $K_h$.[27] These microscopic rate constants for Scheme I are listed in Table III along with values for $k_1$ ($=Q_fk_{-1}$) and the corresponding activation parameters obtained from plots of ln $(k/T)$ vs. $T^{-1}$.

Due to problems with ligand solubility and a tendency to form bis and tris complexes, the thiohydroxamic acid system was investigated in 5% $MeOH/H_2O$ at pseudo-first-order conditions ($[Fe(III)] > 10[HSA]$). In order to verify the validity of comparing data obtained for the hydroxamic acid system by relaxation methods in aqueous solution with kinetic data obtained by pseudo-first-order methods in 5% $MeOH/H_2O$ for the thiohydroxamic acid system, a limited number of experiments were performed with the hydroxamic acid system in aqueous and 5% $MeOH/H_2O$ solutions at pseudo-first-order conditions. A comparison of rate data obtained in these various ways for the hydroxamate system is presented in Figure 2, illustrating the validity of using different experimental conditions to obtain kinetic results for the hydroxamic oxo and thio acids.

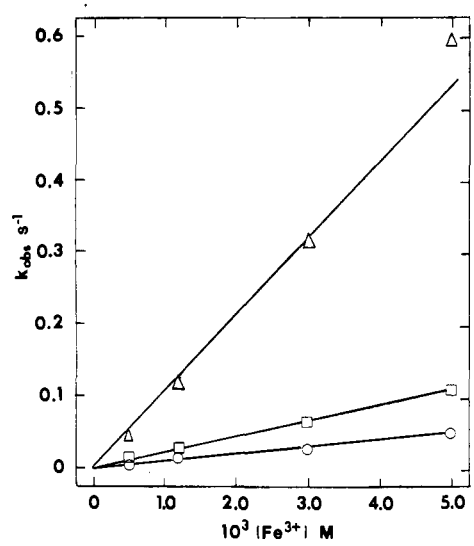


**Figure 3.** Plot of the pseudo-first-order rate constant, $k_{obsd}$, as a function of [Fe(III)] for reaction 1 with $CH_3OC_6H_4C(S)N(OH)H$. Conditions: 25 °C, $I = 2.00$ M ($NaClO_4/HClO_4$), 5% $MeOH/H_2O$. Key: Δ, $[H^+] = 0.0631$ M; O, $[H^+] = 0.8317$ M; □, $[H^+] = 0.316$ M.

From the mechanism shown in Scheme I, the expression (12) for the pseudo-first-order rate constant for mono(thiohydroxamato)iron(III) complex formation can be derived. Plots

$$k_{obsd} = [k_1 + k_2K_h/[H^+]][Fe(III)] + k_{-2} + k_{-1}[H^+] \quad (12)$$

of $k_{obsd}$ vs. [Fe(III)] such as that shown in Figure 3 at a fixed $[H^+]$ are linear as expected from eq 12. The slope corresponds to the sum of the forward rate constants ($k_1 + k_2K_h/[H^+]$) and the intercept the sum of the reverse rate constants ($k_{-2} + k_{-1}[H^+]$). From the intercepts of the plots shown in Figure 3 it is evident that at pseudo-first-order conditions the reverse reaction rate is negligibly small.[29] Consequently, the sum of the forward rate constants may be obtained from the pseudo-first-order rate constant as follows:

$$k_{obsd}/[Fe(III)] = k_1 + k_2K_h/[H^+] \quad (13)$$

Values for $k_1$ and $k_2$ (Scheme I; X = S) were obtained from plots of eq 13 as shown in Figure 4. Values for $k_1$ and $k_2$ at 25 °C are listed in Table III along with the associated activation parameters obtained from plots of ln $k/T$ vs. $T^{-1}$ over the temperature range from 20 to 40 °C. Also included are values for $k_{-1}$ and $k_{-2}$ obtained from $Q_f$ and $Q_f''$ values and their associated activation parameters.

## Discussion

Reaction Scheme I adequately describes a parallel-path mechanism for mono(ligand) complex formation for both the

(29) For example at $[H^+] = 0.316$ M the intercept in Figure 3 is 5 (5) × $10^{-4}$ $s^{-1}$. This is in excellent agreement with the value of $8.1 \times 10^{-4}$ $s^{-1}$ calculated from $k_{-2} + k_{-1}[H^+]$ with the data in Table III.

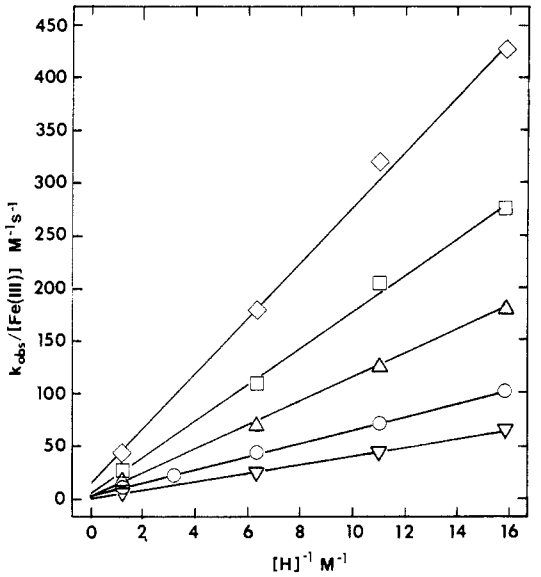


**Figure 4.** Plot of $k_{obsd}/[Fe(III)]$ vs. $[H^+]^{-1}$ for reaction 1 with $CH_3OC_6H_4C(S)N(OH)H$. Conditions: [Fe(III)] = $1.2 \times 10^{-3}$ M; [HSA] = $1.2 \times 10^{-4}$ M; $I$ = 2.00 M ($NaClO_4/HClO_4$); 5% MeOH/$H_2O$. Key: ▽, 20 °C; ○, 25 °C; △, 30 °C; □, 35 °C; ◇, 40 °C.

hydroxamic oxo and thio acid systems. The correlations illustrated in Figures 5 and 6 support a common mechanism for iron(III) complexation and dissociation by both ligands. The isokinetic plots[30] in Figure 5 are defined for both path 1 and path 2 by $CH_3OC_6H_4C(O)N(OH)H$ and 16 other hydroxamic acids[10,12] over a wide range of $\Delta H^*$ and $\Delta S^*$ values. The activation parameters for the reaction of $CH_3OC_6H_4C(S)N(OH)H$ with $Fe_{aq}^{3+}$ fall on these lines within experimental error. An isokinetic plot for a homologous series of reactions implies the same reaction mechanism for each member of the series.[35] The linear correlation between $k_{-1}$ and $k_{-2}$, which is followed by $CH_3OC_6H_4C(O)N(OH)H$ and the other 16 hydroxamic acids[10,12] reported from our laboratory (Figure 6), is also valid for $CH_3OC_6H_4C(S)N(OH)H$. This linear relationship with slope 1 is expected for a ligand-dissociation reaction where the transition states of parallel paths differ by a $H^+$.[36]

We have proposed that mono(hydroxamato)iron(III) complex formation and dissociation proceeds by an associative interchange ($I_a$) mechanism for path 1 and also for path 2 in Scheme I, although in the latter case the associative character may be due to a H-bonded preequilibrium step as shown in Scheme II rather than entering ligand bond formation at iron(III) in the transition state. We have also proposed that initial bond formation occurs at the carbonyl oxygen atom. A detailed discussion of these mechanistic assignments is given elsewhere.[12] The direct comparison of results reported here for the hydroxamic oxo and thio acids is consistent with, and further confirms, these mechanistic interpretations.

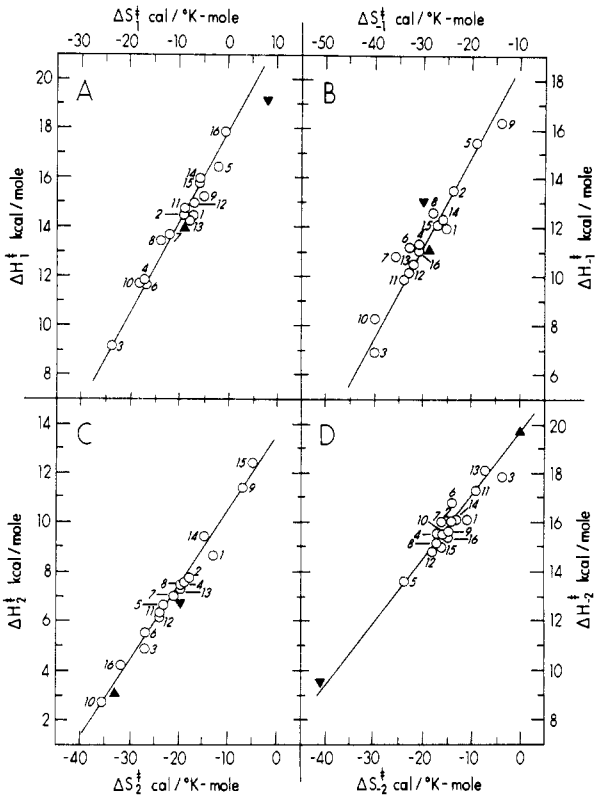


**Figure 5.** Isokinetic plots for the forward and reverse directions: path 1, (A) $\Delta H_1^*$ vs. $\Delta S_1^*$ and (B) $\Delta H_{-1}^*$ vs. $\Delta S_{-1}^*$; path 2, (C) $\Delta H_2^*$ vs. $\Delta S_2^*$ and (D) $\Delta H_{-2}^*$ vs. $\Delta S_{-2}^*$. Key: ▲, $CH_3OC_6H_4C(O)N(OH)H$; ▼, $CH_3OC_6H_4C(S)N(OH)H$. Data points 1–16 are from ref 10 and 12 and are defined for the hydroxamic acids $R_1C(O)N(OH)R_2$ as follows: ((no.) $R_1$, $R_2$): (1) $C_6H_5$, H; (2) $C_6H_5$, $C_6H_5$; (3) $CH_3$, H; (4) $CH_3$, $CH_3$; (5) $C_6H_5$, $CH_3$; (6) 4-$CH_3C_6H_4$, $CH_3$; (7) 4-$CH_3OC_6H_4$, $CH_3$; (8) 4-$NO_2C_6H_4$, $CH_3$; (9) $CH_3$, $C_6H_5$; (10) $CH_3$, 4-$CH_3C_6H_4$; (11) $CH_3$, 3-$IC_6H_4$; (12) $CH_3$, 4-$IC_6H_4$; (13) $CH_3$, 4-$ClC_6H_4$; (14) $CH_3$, 3-$NCC_6H_4$; (15) $CH_3$, 4-$CH_3C(O)C_6H_4$; (16) $CH_3$, 4-$NCC_6H_4$.

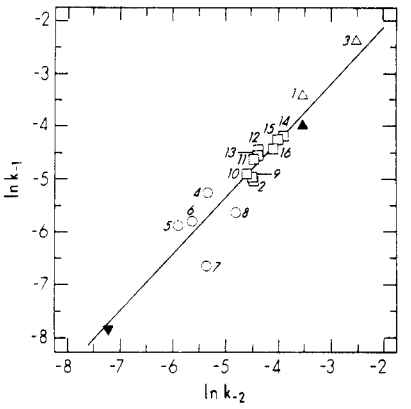


**Figure 6.** Plot of ln $k_{-1}$ (reverse of reaction 7) vs. ln $k_{-2}$ (reverse of reaction 9) at 25 °C. Key: ▲, $Fe(H_2O)_4(CH_3OC_6H_4C(O)N(O)H)^{2+}$; ▼, $Fe(H_2O)_4(CH_3OC_6H_4C(S)N(O)H)^{2+}$. Numbered data points are for the mono(hydroxamato)iron(III) complexes, $Fe(H_2O)_4(R_1C(O)N(O)R_2)^{2+}$, taken from ref 10 and 12 and are defined in the legend for Figure 5. Key: △, hydroxamic acids where $R_2$ = H; □, hydroxamic acids where $R_2$ = substituted phenyl; ○, hydroxamic acids where $R_2$ = $CH_3$.

The $k_1$ and $k_2$ values (Table III) are essentially the same for $CH_3OC_6H_4C(O)N(OH)H$ and $CH_3OC_6H_4C(S)N(OH)H$. This is consistent with compensating $\Delta H^*$ and $\Delta S^*$ values as shown in Figure 5, which would tend to diminish any differences between the corresponding rate constants for the two ligands.[30] Furthermore, the ratio $k_2/k_1$ varies from 530 to 1150 for both ligands, which is in the range for the ratio of water-exchange rate constants for $Fe(H_2O)_5OH^{2+}$ and $Fe(H_2O)_6^{3+}$ ($k_{ex}(Fe(H_2O)_5OH^{2+})/k_{ex}(Fe(H_2O)_6^{3+})$ = 750).[37] This is consistent with an interchange

(30) The linear correlations between $\Delta H^*$ and $\Delta S^*$ shown in Figure 5 do not conform to the strict statistical criteria established by Krug[31] and Exner[32] for a true isokinetic relationship. However, we have applied the error analysis described by Petersen et al.[33] and Wiberg[34] to these data that shows that the $\Delta H^*$ and $\Delta S^*$ ranges observed are statistically significant and the linear correlations valid. Consequently, the range and number of data points for each correlation are sufficiently large for us to suggest that a compensating effect is operating for both path 1 and path 2.

(31) Krug, R. R. *Ind. Eng. Chem. Fundam.* **1980**, *19*, 50.
(32) Exner, O. *Collect. Czech. Chem. Commun.* **1972**, *37*, 1425; **1975**, *40*, 2762; *Progr. Phys. Org. Chem.* **1973**, *10*, 411.
(33) Petersen, R. C.; Markgraf, J. H.; Ross, S. D. *J. Am. Chem. Soc.* **1961**, *83*, 3819.
(34) Wiberg, K. B. "Physical Organic Chemistry"; Wiley: New York, 164; pp 376–379.
(35) Wilkins, R. G. "The Study of Kinetics and Mechanism of Reactions of Transition Metal Complexes"; Allyn and Bacon: Boston, 1974.
(36) Asher, L. E.; Deutsch, E. *Inorg. Chem.* **1973**, *12*, 1774.

**Scheme II**

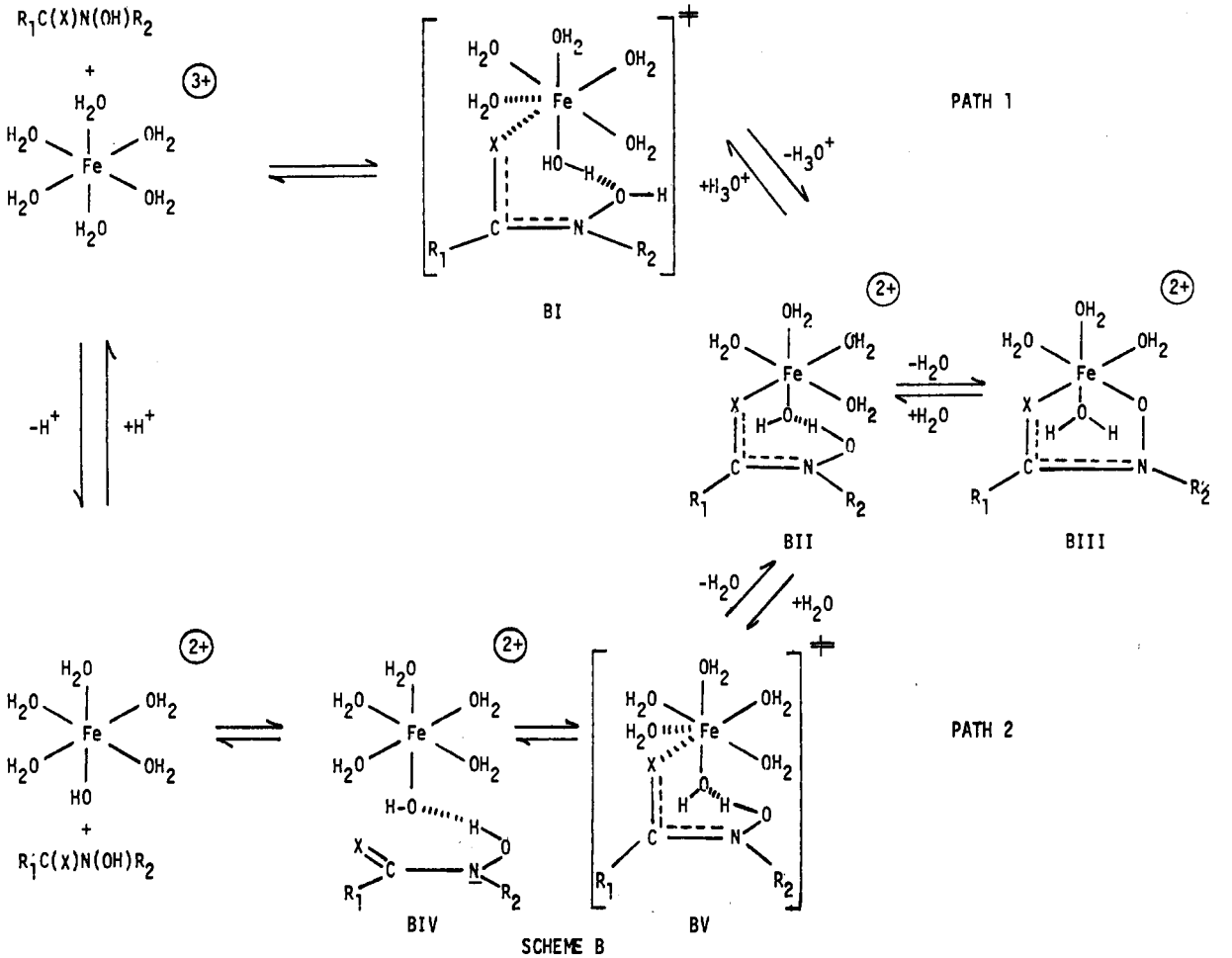


SCHEME B

mechanism where the energetics are dominated by $H_2O$ ligand dissociation. The significant difference in activation parameters (Table III) between $CH_3OC_6H_4C(O)N(OH)H$ and $CH_3OC_6H_4C(S)N(OH)H$, however, is consistent with some entering ligand participation in the transition state for complex formation. It has been proposed that the more associative a nucleophilic ligand substitution reaction, the lower the expected $\Delta H^{\ddagger}$ value.[38] A comparison of $\Delta H_1^{\ddagger}$, $\Delta H_2^{\ddagger}$, $\Delta S_1^{\ddagger}$, and $\Delta S_2^{\ddagger}$ for $CH_3OC_6H_4C(O)N(OH)H$ and $CH_3OC_6H_4C(S)N(OH)H$ shows smaller $\Delta H^{\ddagger}$ and more negative $\Delta S^{\ddagger}$ values for the hydroxamic oxo acid. Furthermore, the $\Delta H_1^{\ddagger}$ and $\Delta H_2^{\ddagger}$ values for both ligands are less than, or comparable to, the corresponding $\Delta H^{\ddagger}$ values for $Fe_{aq}^{3+}$ water exchange.[37,39] These observations are consistent with an $I_a$ mechanism with initial bond formation at >C=X (X = S, O; Scheme II) and the expectation that an X = O donor should be more nucleophilic toward the hard iron(III) center than an X = S donor.

The stability constants for both path 1 and path 2 (Scheme I) are greater for the thiohydroxamic acid ligand than for the hydroxamic acid ligand. This could be due in part to the much lower $pK_a$ of the thiohydroxamic acid that results in less competition from $H^+$ in complex formation. The thiohydroxamate anion forms a less stable complex with iron(III) than the corresponding hydroxamate anion, as might be expected from consideration of the hard/soft acid/base principle. At physiological pH, mono(ligand)iron(III) complex formation occurs to a greater extent for the thiohydroxamic acid ligand.

A significant difference between the hydroxamic oxo and thio acid ligands described here is the rate of ligand dissociation by the acid-dependent (path 1) and acid-independent (path 2) paths. The ligand-dissociation rate constant for either path is smaller by a factor of ca. 50 for $Fe(H_2O)_4(CH_3OC_6H_4C(S)N(O)H)^{2+}$ relative to $Fe(H_2O)_4(CH_3OC_6H_4C(O)N(O)H)^{2+}$ (Table III). Furthermore, the thiohydroxamic acid ligand $CH_3OC_6H_4C(S)N(OH)H$ has dissociation rate constants 10–235 times smaller than any of the 16 hydroxamic acids investigated in our laboratory (Figure 6). A possible explanation for the enhanced kinetic stability of the thiohydroxamic acid over the hydroxamic acid may be seen by considering the resonance forms II–IV. Assuming

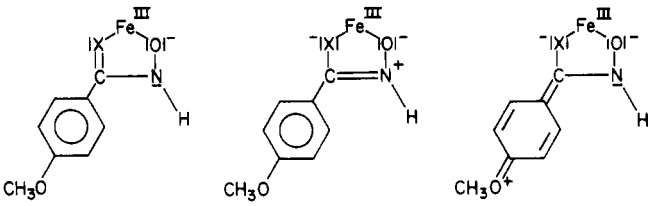

II III IV

the validity of our arguments concerning initial bond formation at >C=X and invoking the principle of microscopic reversibility, a buildup of formal negative charge on X will result in a smaller dissociation rate constant. This may be achieved by delocalization of the N atom lone pair of electrons into the C–N bond as shown in III.[40] Barriers to C–N bond rotation in amides and the corresponding thioamides,[41–44] and hydroxamate oxo and thio

(37) Dodgen, H. W.; Liu, G.; Hunt, J. P. *Inorg. Chem.* **1981**, *20*, 1002.
(38) Tanaka, M. *Inorg. Chim. Acta* **1981**, *54*, 129.
(39) Grant, M.; Jordan, R. B. *Inorg. Chem.* **1981**, *20*, 55.

(40) See ref 12 and references cited therein for a discussion of structural evidence supporting partial C–N double-bond character in coordinated hydroxamic acids. The molecular structure of tris(*N*-methylformothiohydroxamato)iron(III) determined by X-ray diffraction suggests partial C–N double-bond character for the coordinated thiohydroxamic acid.[21]
(41) Sandström, J. *Tetrahedron Lett.* **1979**, 639.
(42) Walter, W.; Schaumann, E.; Voss, J. *Org. Magn. Reson.* **1971**, *3*, 733.

esters,[45] are found to be higher for the thio compounds. This suggests an increased contribution from resonance form III when X = S. Further support comes from a comparison of bond lengths in the tris(hydroximato) and -(thiohydroximato) complexes of chromium(III), where the C-N bond distance in the thio compound is somewhat shorter than found for the O compound.[46,47]

It is interesting to note that the rate constants for the dissociation of the last hydroxamate group of the siderophore ferrioxamine B from iron(III) by acid-dependent and acid-independent paths also follow the correlation shown in Figure 6 but are larger than the values found for $Fe(H_2O)_4(CH_3OC_6H_4C(S)N(O)H)^{2+}$.[48,49] The kinetic and thermodynamic stability of the thiohydroxamic acid ligand studied here suggests that the thiohydroxamates may also serve a biological function as an iron(III) chelator and that future research may establish the existence of a thiohydroxamate-based siderophore.

**Acknowledgment** is made to the donors of the Petroleum Research Fund, administered by the American Chemical Society, for support of this research. We thank C. P. Brink for a sample of the hydroxamic acid and for helpful discussions and A. B. Griffis for preliminary synthetic work with thiohydroxamic acids.

**Registry No.** I (X = O), 94944-52-2; I (X = S), 94944-53-3; $Fe(H_2O)_6^{3+}$, 15377-81-8; $Fe(H_2O)_5OH^{2+}$, 15696-19-2; $4\text{-}CH_3OC_6H_4C(O)N(OH)H$, 10507-69-4; $4\text{-}CH_3OC_6H_4C(S)N(OH)H$, 17650-20-3.

**Supplementary Material Available:** Rate constant data (Table II) (4 pages). Ordering information is given on any current masthead page.

(43) Bernardi, F.; Lunazzi, L.; Zanivato, P. *Tetrahedron* **1977**, *33*, 1337.
(44) Piccini-Leopardi, C.; Fobre, O.; Zimmermann, D.; Reisse, J. *Can. J. Chem.* **1977**, *55*, 2649.
(45) Walter, W.; Schaumann, E. *Justus Liebigs Ann. Chem.* **1971**, *743*, 154.
(46) Abu-Dari, K.; Freyberg, D.; Raymond, K. N. *Inorg. Chem.* **1979**, *18*, 2427.
(47) Abu-Dari, K.; Raymond, K. N. *Inorg. Chem.* **1980**, *19*, 2034.
(48) Monzyk, B.; Crumbliss, A. L. *Inorg. Chim. Acta, Bioinorg. Sect.* **1981**, *55*, 25.
(49) Monzyk, B.; Crumbliss, A. L. *J. Am. Chem. Soc.* **1982**, *104*, 4921.

Contribution from the EMCA Division of RHAMCO, Mamaroneck, New York 10543, and Departments of Chemistry, University of Delaware, Newark, Delaware 19716, and University of Rhode Island, Kingston, Rhode Island 02881

# Octahedral Dialkyltin Complexes: A Multinuclear NMR Spectral Solution Structural Study

WILMONT F. HOWARD, JR.,[†] ROGER W. CRECELY,[‡] and WILFRED H. NELSON*[§]

*Received February 3, 1984*

Octahedral dialkyltin complexes of type $R_2SnCh_2$ (R = alkyl, Ch = bidentate ligand) yield NMR tin-carbon $|^1J(^{119}Sn-^{13}C)|$ and tin-hydrogen, $|^2J(^{119}Sn-C-^1H)|$ coupling constants that allow the estimation of C-Sn-C bond angles. Complexes with β-keto enolate ligands show trans alkyl structure with calculated ∠C-Sn-C between 174 and 180°. Very nearly cis arrangements with ∠C-Sn-C between 109 and 126° characterize the 8-hydroxyquinolinolates. The sterically crowded 2-methyl-8-hydroxyquinolinolate family shows intermediate skew-cis structures. Skew (i.e., trapezoidal bipyramidal) frameworks were found for tropolonates and 1-picolinates. Finally, $^{119}Sn$ NMR spectra have been analyzed to yield $|^3J(^{119}Sn-C-C-^1H)|$ values for the first time in octahedral species. Syntheses of eight new benzoylacetonate, 2-methyl-8-hydroxyquinolinolate, and tropolonate derivatives are reported.

## Introduction

Even though it might appear that the structures of six-coordinate $R_2SnCh_2$ species should be simple octahedra, 20 years of structural investigations have shown a substantially different picture. Most early studies interpreted results on the basis of simple trans or cis structures,[1-7] and, indeed, there is little doubt that some structures are trans in solution[8,9] and the solid state.[10] Others certainly are cis.[11,12] More recently, Kepert[13] noted that many octahedral organometallic complexes, including several tin complexes, are of neither regular cis nor regular trans geometry, but that an intermediate geometry, skew or trapezoidal bipyramidal, is more stable (see Figure 1; skew structures have C-Sn-C angles of 135-155°). We have shown[14] by means of the Kerr effect that a number of structures previously believed to be trans are better described as skew in solution. Extensive studies involving dipole moments,[15] IR spectroscopy,[16] and depolarized light scattering[17-19] are better interpreted in terms of distorted structures rather than cis-trans mixtures.

Early proton NMR studies[15,20-22] showed little evidence for cis-trans equilibria. Although information concerning the mechanism of ligand exchange has been obtained, such studies have shown primarily that ligand exchange is very rapid. More recent $^{119}Sn$ and $^{13}C$ NMR experiments by Otera[23,24] indicate that NMR may provide a more useful means of probing the configurations of $R_2SnCh_2$-type complexes.

Much interesting Mössbauer data are available. Quadrupole splittings from $^{119}Sn$ Mössbauer spectra are related to molecular geometry in octahedral complexes and have been used to calculate

[†] EMCA Division of RHAMCO.
[‡] University of Delaware.
[§] University of Rhode Island.

(1) McGrady, M. M.; Tobias, R. S. *Inorg. Chem.* **1964**, *3*, 1960.
(2) McGrady, M. M.; Tobias, R. S. *J. Am. Chem. Soc.* **1965**, *87*, 1909.
(3) Barbieri, R.; Faroglia, G.; Gustiniani, M.; Roncucci, L. *J. Inorg. Nucl. Chem.* **1964**, *26*, 203.
(4) Roncucci, L.; Faroglia, G.; Barbieri, R. *J. Organomet. Chem.* **1964**, *1*, 427.
(5) Nelson, W. H.; Martin, D. F. *J. Organomet. Chem.* **1965**, *27*, 89.
(6) Tanaka, T.; Komura, M.; Kawasaki, Y.; Okawara, R. I. *J. Organomet. Chem.* **1964**, *1*, 484.
(7) Veeda, R.; Kawasaki, Y.; Takara, T.; Okawara, R. I. *J. Organomet. Chem.* **1966**, *5*, 1964.
(8) Ramos, V. B.; Tobias, R. S. *Spectrochim. Acta, Part A* **1973**, *29A*, 953.
(9) Ramos, V. B.; Tobias, R. S. *Spectrochim. Acta, Part A* **1974**, *30A*, 181.
(10) Miller, G. A.; Schlemper, E. O. *Inorg. Chem.* **1973**, *12*, 677.
(11) Schlemper, E. O. *Inorg. Chem.* **1967**, *6*, 2012.
(12) Nelson, W. H.; Aroney, M. J. *Inorg. Chem.* **1973**, *12*, 132.
(13) Kepert, D. L. *Inorg. Chem.* **1977**, *12*, 1.
(14) Brahma, S. K.; Nelson, W. H. *Inorg. Chem.* **1982**, *21*, 4076.
(15) Moore, C. Z.; Nelson, W. H. *Inorg. Chem.* **1969**, *8*, 138.
(16) LeBlanc, R.; Nelson, W. H. *J. Organomet. Chem.* **1976**, *113*, 257.
(17) Asting, N.; Nelson, W. H. *Inorg. Chem.* **1977**, *16*, 148.
(18) Nelson, W. H.; Howard, W. F., Jr.; Pecora, R. *Inorg. Chem.* **1982**, *21*, 1483.
(19) Howard, W. F., Jr.; Nelson, W. H. *Inorg. Chem.* **1982**, *21*, 2283.
(20) Jones, R. W.; Fay, R. C. *Inorg. Chem.* **1973**, *12*, 2599.
(21) Serpone, N.; Hersh, K. A. *Inorg. Chem.* **1974**, *13*, 2091.
(22) Nelson, W. H. *Inorg. Chem.* **1967**, *6*, 1509.
(23) Otera, J.; Hinoishi, T.; Kawabe, Y.; Okawara, R. *Chem. Lett.* **1981**, 273.
(24) Otera, J. *J. Organomet. Chem.* **1981**, *221*, 57.

0020-1669/85/1324-2204$01.50/0 